Article

Development of Quercetin Micellar Nanogel: Formulation, Characterization, and *In Vitro* Cytotoxocity Study

Harshad S. Kapare [1,*], Sunil Kanadje [1], Prabhanjan Giram [1,2,*], Aditi Patil [1] and Ritesh P. Bhole [1,3]

1   Dr. D. Y. Patil Unitech Society's, Dr. D. Y. Patil Institute of Pharmaceutical Sciences & Research Pimpri, Pune 411018, Maharashtra, India
2   Department of Pharmaceutical Sciences, The State University of New York, Buffalo, NY 14214, USA
3   Dr. D. Y. Patil Dental College and Hospital, Dr. D. Y. Patil Vidyapeeth, Pimpri, Pune 411018, Maharashtra, India
*   Correspondence: hskapare@yahoo.in (H.S.K.); prabhanjanpharma@gmail.com (P.G.)

Abstract: Quercetin, a flavonoid, has well-proven cytotoxicity potential, but its therapeutic efficacy is hampered by hydrophobicity, stability issues, and lower bioavailability. The present research aims to address these issues and formulation barriers by formulating a quercetin-loaded micellar nanogel. Quercetin was encapsulated in PF 68 micelles to enhance its solubility, loading, and stability to better its therapeutic potential. The nanogel was further characterized regarding for pH, spreadability, and *in vitro* cytotoxicity against human breast cancer cells (MCF-7). The resulting micelles exhibited a particle size of 180.26 ± 2.4 nm, surface charge of -13.5 mV, entrapment efficiency of $78.4 \pm 1.2\%$, and in vitro release of $96.11 \pm 0.75\%$ up to 8 h. This in vitro cytotoxicity study on MCF-7 cell lines reveals the improved TGI and GI 50 values of micellar nanogel formulation compared to quercetin. The overall study results demonstrated that the developed micellar nanogel system might serve as a promising nanocarrier to enhance the cytotoxic potential of quercetin in cancer therapy.

Keywords: anticancer; micelles; MCF-7; nanogel; Pluronic F68; quercetin

1. Introduction

Phytoconstituents are often favored over drugs because of their safety and compatibility with biological systems [1]. However, challenges such as low aqueous solubility, less bioavailability, and instability limit their therapeutic applications by affecting their PK profile. These issues associated with polyherbal formulations demand the development of novel formulations to improve bioavailability and therapeutic benefits [2]. Plant-derived bio-actives like polyphenols and flavonoids have proven promising cytotoxic potential with their widespread abundance in natural products [3]. Natural products exhibit a range of pharmacological effects, including anti-viral, anti-inflammatory, anti-allergic, etc. Various bioactives like quercetin, apigenin, luteolin, etc., face challenges with low bioavailability due to their suboptimal biopharmaceutical properties that make their effective incorporation into drug delivery systems a persistent challenge [4]. To improve therapeutic efficacy, various advanced drug delivery systems, like self-micro-emulsifying delivery system for baicalein, quercetin, and apigenin [4–6], and nanoparticulate systems for genistein, luteolin, and quercetin [7–9] were reported to maximize their therapeutic activity.

Quercetin is a glycoside commonly found in various natural resources [10]. Various mechanistic studies reported the use of quercetin for the suppression of various types of

tumor growth through apoptosis, oxidative stress, proliferation, and metastasis [11]. Mechanistic studies on the inhibitory effects on the expression of mutant p53, [12], oxidative stress [13–15], metastasis [16–18], P-glycoprotein expression [19], irinotecan metabolite (SN-38) with quercetin demonstrated that these effects better improve apoptosis compared to SN-38 alone [20], type II estrogen binding-site-mediated anti-proliferative effects of quercetin [21], pro-apoptotic autophagy, etc. [22]. Despite its well-proven cytotoxic potential, therapeutic applications of quercetin are restricted with factors like less bioavailability, lipophilicity, rapid metabolism, and unfavorable PK [23,24]. Various formulation strategies are attempted to address these challenges, including micro-emulsions, phytosomal delivery, micellar drug delivery, solid lipid nanoparticles (SLNs), liposomes, etc. [25–30]. However, these approaches lack detailed investigation in terms of the optimization of material attributes, process parameters, characterization, and pharmacological activities that are important for successful formulation development.

Quercetin, a flavonoid with significant antioxidant and anti-inflammatory properties, has shown promise in cancer therapy but faces challenges related to its low aqueous solubility, rapid metabolism, and limited bioavailability, which hinder its clinical translation [31]. In breast cancer, studies suggest that quercetin induces apoptosis by modulating pathways such as PI3K/Akt and NF-κB, but its efficacy is influenced by the tumor microenvironment and pharmacokinetic constraints [32]. Compared to other cancers, such as prostate and colorectal cancers, where quercetin demonstrates robust anti-proliferative effects due to higher intracellular uptake and stability, its therapeutic potential in breast cancer remains less explored [33]. These challenges necessitate the development of advanced delivery systems, such as micellar nanogels, to enhance their solubility, stability, and targeted delivery to breast cancer cells [34].

Micelles are amphiphilic structures composed of molecules with both hydrophobic and hydrophilic regions. At and above the critical micellar concentration (CMC), micelles start to demonstrate aggregation [35,36]. Polymeric micellar drug delivery showed potential for delivering their payloads through an enhanced permeability and retention (EPR) effect, which plays an important role in the passive targeting of, e.g., tumor tissues. Polymeric micelle-based drug delivery systems for topical application need to attempt to improve the localization and permeation of drugs in anon-invasive manner [37–40]. In our previous study, we developed quercetin-loaded liposomes and nanocochleates for improving PK profiles, resulting in improved solubility, stability, and anticancer activity. In our other findings, we synthesized and formulated LHRH-conjugated PEGylated PLGA nanocapsules loaded with quercetin with docetaxel in prostate cancer treatment [41,42]. Based on this work, we now use quercetin in the development of nanogels for evaluating its potential against breast cancer. The present study aimed to develop and optimize micellar gel-based drug delivery systems for quercetin to develop the suitable dosage form, localization, and cytotoxicity of quercetin.

2. Materials and Methods

2.1. Materials

Quercetin, Pluronic F-68 (PF-68), was procured from HiMedia, Labs Pvt. Ltd., Mumbai, India. The dialysis bag (molecular weight cut off 12,000) was procured from Sigma-Aldrich Chemical Private Ltd. (Bangalore, India). All other solvents used for this study were of analytical grade.

2.2. Formulation Development

Micelles were formulated using a thin-film hydration method. Quercetin and PF-68 were precisely weighed and dissolved in ethanol (15 mL) in RBF and evaporated with a

vacuum rotary evaporator to remove organic solvent at 55 °C for 15 min. The resulting thin film was further hydrated with distilled water to obtain micellar structures. The quercetin-loaded micelles were subjected to lyophilization (Lyophilizer, Martin Christ, Alpha 2-4 LSC Basic). Mannitol (5%) was used as a cryoprotectant to preserve the structure [38].

2.3. Optimization

A 3^2 factorial design was applied based on the preliminary trial batches to carry out 9 experimental runs to understand the impact of independent variables, as shown in Table 1. The amount of PF68 (X1) and rotation speed (X2) were identified as independent variables to study the impact on size and encapsulation [39]. Micellar size and percent encapsulation were identified as dependent variables.

Table 1. Details of experimental runs and responses using 3-level factorial design.

Batches	Coded Levels		Actual Levels		Response		
	X1	X2	X1 (mg)	X2 (rpm)	Micellar Size (nm)	Entrapment Efficiency (%)	Surface Charge Value (mV)
F1	0	1	150	100	216.13 ± 1.9	73.20 ± 0.8	−13.9 ± 0.019
F2	0	0	150	75	180.26 ± 2.4	78.40 ± 1.1	−13.5 ± 0.024
F3	1	0	200	75	157.30 ± 2.1	76.22 ± 1.2	−14.2 ± 0.041
F4	−1	−1	100	50	224.30 ± 2.2	73.20 ± 0.8	−13.7 ± 0.014
F5	−1	1	100	100	209.10 ± 2.1	72.25 ± 1.1	−13.5 ± 0.018
F6	0	−1	150	50	218.30 ± 2.4	78.40 ± 1.2	−13.9 ± 0.022
F7	1	−1	200	50	229.80 ± 2.1	78.33 ± 1.2	−14.4 ± 0.028
F8	−1	0	100	75	159.50 ± 2.3	74.53 ± 0.9	−13.2 ± 0.020
F9	1	1	200	100	195.15 ± 1.8	72.30 ± 0.9	−13.9 ± 0.025

2.4. Micellar Size and PDI Zeta Potential Analysis

The micellar size was determined with a Horiba SZ-100 particle size analyzer, which works on the principle of dynamic light scattering. The samples were suitably diluted, and the Z-average and PDI were calculated at a 90° scattering angle (*n*=3) [40]. Surface charge was determined to understand colloidal stability. The zeta potential was analyzed by using Horiba SZ-100 at a temperature of 25 °C [40].

2.5. Entrapment Efficiency (%EE)

Entrapment efficiency was measured by dissolving micelles in ethanol. Absorbance was measured at 373 nm on UV-1800 Shimadzu after filtering through a 0.45 μm membrane filter. The % EE was determined by the following equation:

$$\% \text{ EE} = (\text{Amount of drug encapsulated})/(\text{Total amount of drug added}) \times 100$$

2.6. Differential Scanning Colorimetry (DSC) and FTIR

DSC studies of lyophilized quercetin micelles were carried out using DSC-Hitachi 7020 to understand the molecular dispersion of quercetin in micelles. The sample was appropriately weighed, transferred into an aluminum pan, and determined with the 10 °C/min heating rate set to 30 to 350 °C, and DSC thermograms were obtained for quercetin, PF-68, and the formulation [36,41]. The FTIR studies of quercetin, PF-68 and formulation were performed using FTIR-Shimadzu, 8400 S, Japan. FTIR spectra were recorded at 400 to 4000 cm^{-1} to understand the molecular dispersion of quercetin in micelles [40,41].

2.7. Morphology Study

The morphology of the developed formulation was observed with photographs recorded with a TEM microscope at 200 kV. Carbon-coated copper grid was used to form the thin film [37].

2.8. In Vitro Cytotoxicity Study

The *in vitro* cytotoxicity study was conducted to assess the cytotoxic effects of quercetin and developed formulation on human breast cancer MCF-7 cells using Sulforhodamine B assay (SRB assay). This study was carried out at concentrations of 10 μg/mL, 20 μg/mL, 40 μg/mL, and 80 μg/mL. Then, 50% growth inhibition (GI50) and the total growth inhibition (TGI) of drug concentration were measured [42,43].

2.9. Formulation of Quercetin Micellar Nanogel

Carbopol 940 (1 g) was added to 10 mL of developed micelle formulation using a mechanical shaker for 30 min and left for polymer swelling. Triethanolamine was used to maintain the pH of gel [44,45].

2.10. Characterization of Quercetin Micellar Nanogel

The pH of the quercetin-loaded micellar gel was determined using a pH meter by dipping the electrode into the gel and allowing it to equilibrate before measuring with a calibrated pH meter set to 25 °C [45]. Micellar gel (1 g) was placed between two slides, and a weight of 100 g was applied for 5 min to form a uniform layer. The time required to separate the two glass slides was used to calculate spreadability [45]. The viscosity of the quercetin nanogel was measured by using a Brookfield viscometer using spindle no 6 with 10 rpm [45]. The release pattern of quercetin from the developed dosage form was evaluated using the dialysis bag technique in PBS (pH 6.8). The dialysis membrane with a molecular weight cut-off of 12,000 Da was selected for the developed formulation (1 mg equivalent), along with pure quercetin as the control. Then, it underwent continuous magnetic stirring at 100 rpm/min and 37 °C ± 0.5°C and analyzed using UV-1800 Shimadzu at 373 nm [44,45].

3. Results and Discussion

Various trial batches were attempted to understand the impact of varying the PF-68 amount and the rpm as material attributes and process parameters, respectively.

3.1. Formulation Optimization for Quercetin-Loaded Polymeric Micelles

The experimental approach with 3^2 factorial designs was employed for formulation optimization. As shown in Table 1, as per 3^2 factorial designs, the nine batches were formulated and analyzed for size and entrapment efficacy as dependent variables. The data obtained were analyzed and fitted in Design-Expert software version 13. The study results indicated that a quadratic model was observed to be the best fit for size, while a linear model was deemed the most suitable for entrapment efficacy using the following equations:

$$\text{Size} = \pm 171.71 * A\text{-}8.67 * B\text{-}4.86 * AB\text{-}9.04 \pm 49.78B2$$

$$\% \text{ Entrapment Efficiency} = \pm 77.84 \pm 1.15 * A\text{-}2.02 * B\text{-}1.26 * AB\text{-}2.19 * A2\text{-}1.77B2$$

In the above equations, the coded values for the amount of PF 68 and speed of rotation were represented as A and B, respectively. The positive coefficient for the factor in the equation suggests an increase in the response, where negative indicates reduced response value.

3.2. Design of Experimental Approach

Based on the outcomes of the preliminary trial experimental batches, the amount of PF68 (X1) and the speed of rotation evaporator (X2 were deemed as crucial in determining the average size and entrapment efficiency (% EE) of the micelles. The amount of PF-68 was observed to significantly influence the entrapment efficiency, as an optimal polymer concentration above the CMC is essential for micellar formation and drug encapsulation. Additionally, the rotary evaporator speed impacts the film formation from the polymer, affecting its size, thickness, and uniformity of micellar structures.

The results indicated that the optimized formulation with a smaller desirable size and higher entrapment was achieved at a PF-68 amount of 150 mg and rotation speed of 75 rpm. A 3D response surface plot, constructed using Design-Expert software Stat-Ease Version 13 (Figure 1), was used to analyze the interaction between the independent and dependent variables. The 3D plot demonstrated that both PF 68 and rotation speed significantly influenced the average size and entrapment efficacy. The plot indicated that increasing the amount of PF68 led to a decrease in particle size and an increase in % EE, and conversely, reducing had the opposite effect. The rotational speed of the evaporator played a key role in achieving both a smaller size and higher efficacy. Figure 1A,B represent response surface plots showing the effect of formulation and process variables.
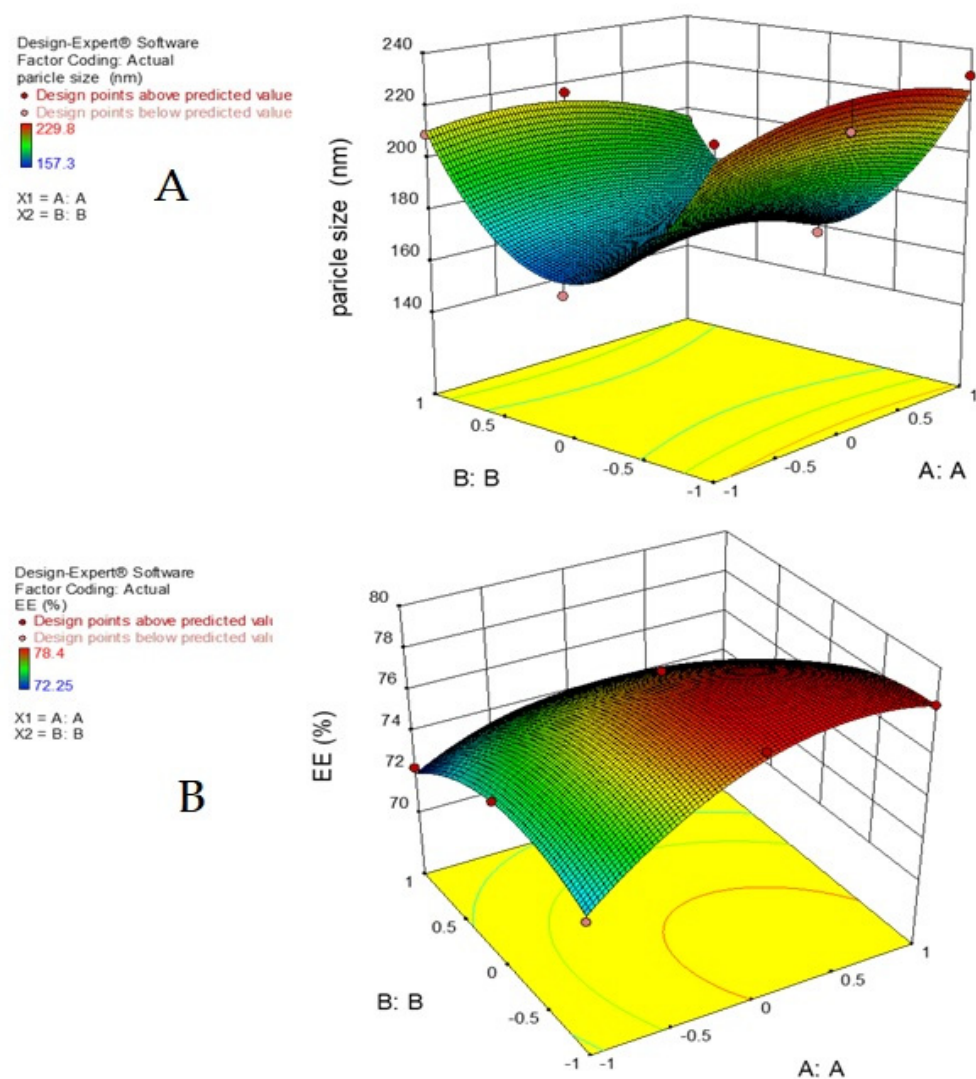

Figure 1. Response surface plots showing the effect of variables on (**A**) particle size and (**B**) % entrapment efficiency.

3.3. Particle Size, Zeta Potential, and Encapsulation Efficiency Analysis

The average-size of optimized formulation (batch F2), as shown in Table 1, with a size and PDI 180.26 ± 2.4 nm and 0.2, respectively (Figure 2A), indicates uniform dispersion. The surface charge of the developed formulation was found to be −13.5 mV (Figure 2B). This charge plays a crucial role in maintaining colloidal stability. In the case of PF-68, surface charge variations may potentially arise from quercetin encapsulation and, to some extent, the adsorption of non-entrapped quercetin in the micelles. The percent entrapment of the formulated quercetin micelle ranged from 72.25 ± 1.1 to 78.40 ± 1.1%, as shown in Table 1.
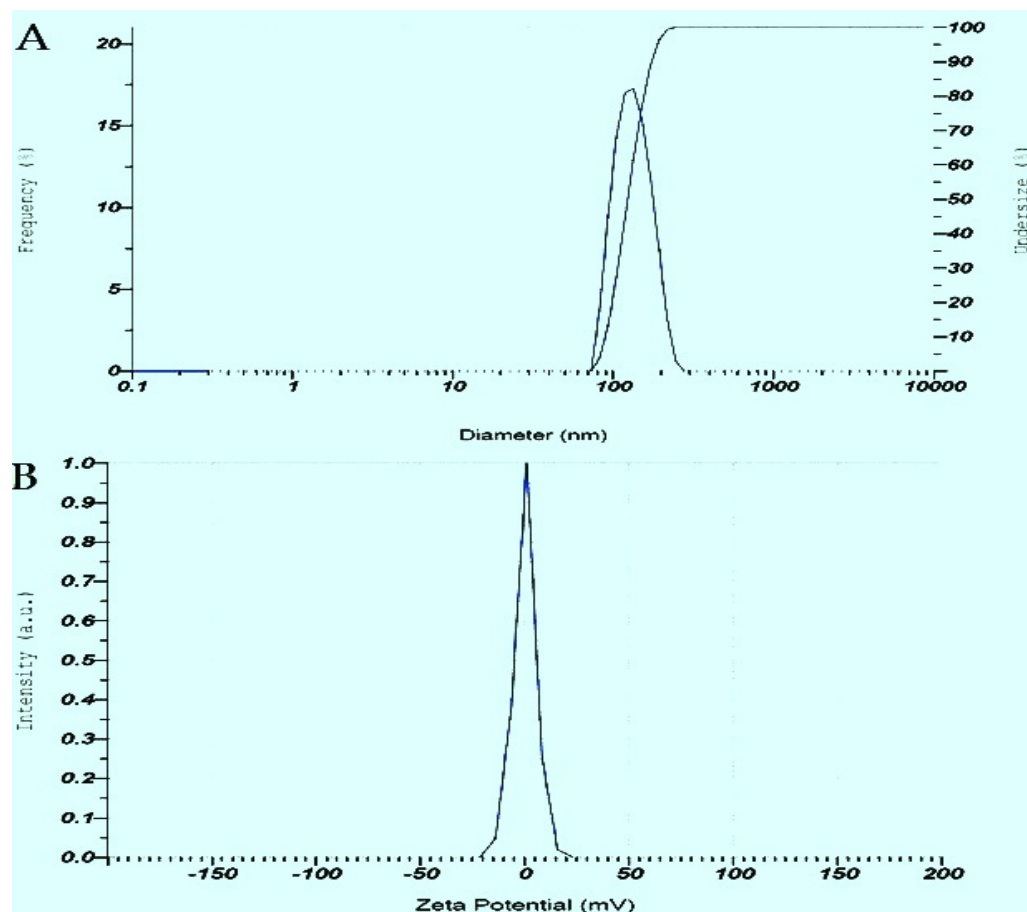

Figure 2. (**A**) Particle size and distribution of quercetin-loaded polymeric micelle, (**B**) zeta potential analysis of quercetin-loaded polymeric micelles.

3.4. DSC and FTIR Studies

DSC thermograms for quercetin, PF 68, and the developed formulation are illustrated in Figure 3. The DSC thermogram of quercetin displayed an endothermic peak at 317.7 °C, and Pluronic F68 at 50 °C, indicating their respective melting points were attributed to their crystalline nature. On the other hand, in the DSC thermogram of the developed formulation, the endothermic peak for quercetin appeared with reduced intensity, confirming the molecular dispersion of quercetin into the micellar structure.
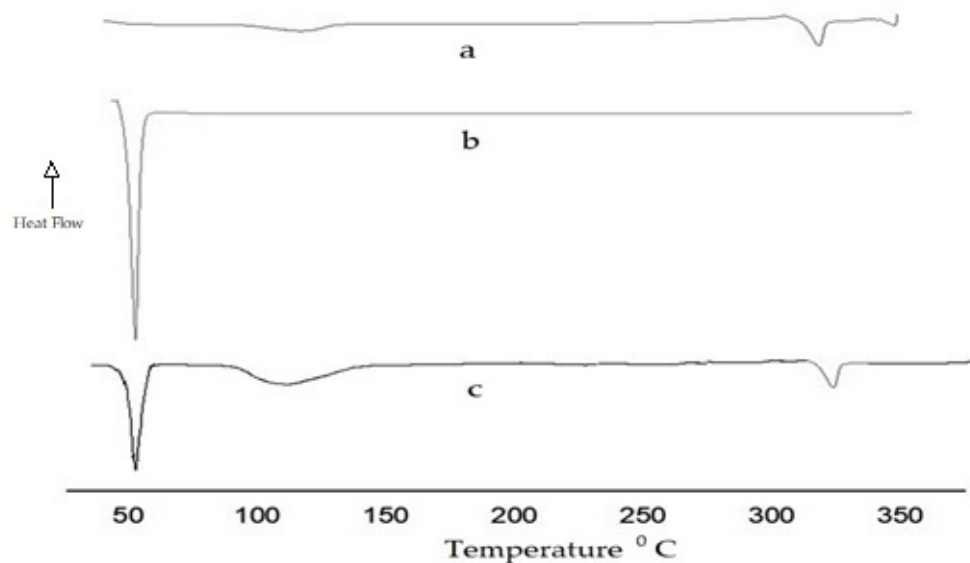
Figure 3. DSC thermogram of (**a**) QCT, (**b**) Pluronic F68, and (**c**) formulation.

FTIR spectra of quercetin, Pluronic F68, and the formulation were compared, as shown in Figure 4. From the FTIR spectra of quercetin, it was observed that the characteristic peaks appear at wavenumbers 3401.35 and 3275.17 cm^1 of O-H stretching, 1663.39 cm^1 for C=O stretching, 15.20.0 and 1563.02 cm^1 for C=C stretching, 1214.56 and 1260.45 cm^1 for C-O stretching, and 841.73 and 864.68 cm^1 forC-H bending.
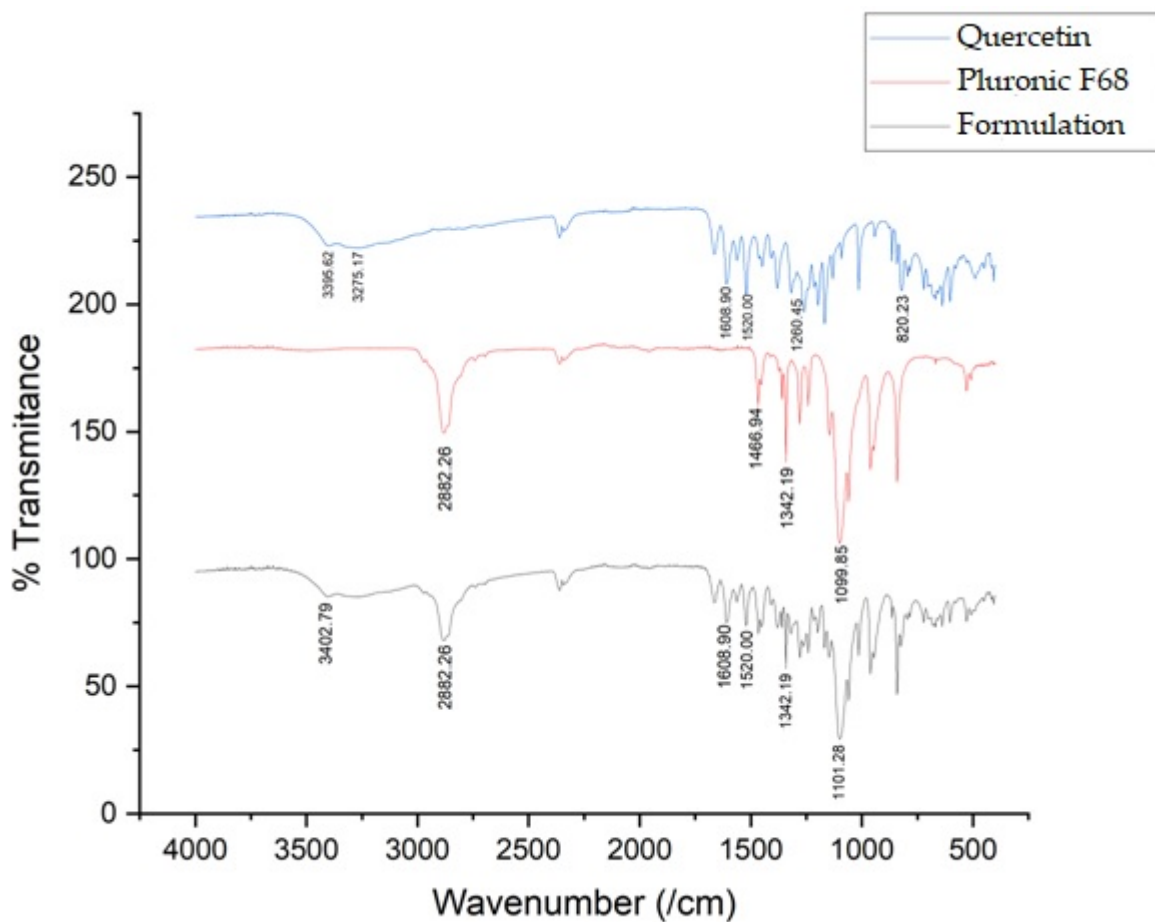

Figure 4. FTIR spectra of quercetin, Pluronic F68, and formulation.

From the FTIR spectra of Pluronic F68, it was observed that the characteristic peaks appear at wavenumbers 2882.26 cm^1 for C-H stretching, 1145.73 cm^1 for C-O-C stretching, 1359.39,1372.30, and 1454.04 cm^1 for C-H bending, and 159.70 and 1099.85 cm^1 for C-O stretching. From the FTIR spectra of the formulation, it was observed that the characteristic peaks of quercetin appear with reduced intensity. The study results regarding the reduced intensity of the quercetin peaks revealed that quercetin could be uniformly dispersed within the micellar core inside a hydrophobic environment.

3.5. Morphology (TEM) Studies

Figure 5A,B represent the morphological structure of micelles. The results revealed that the developed quercetin micelles are spherical and uniform with a smooth surface, and no drug crystallization was observed.
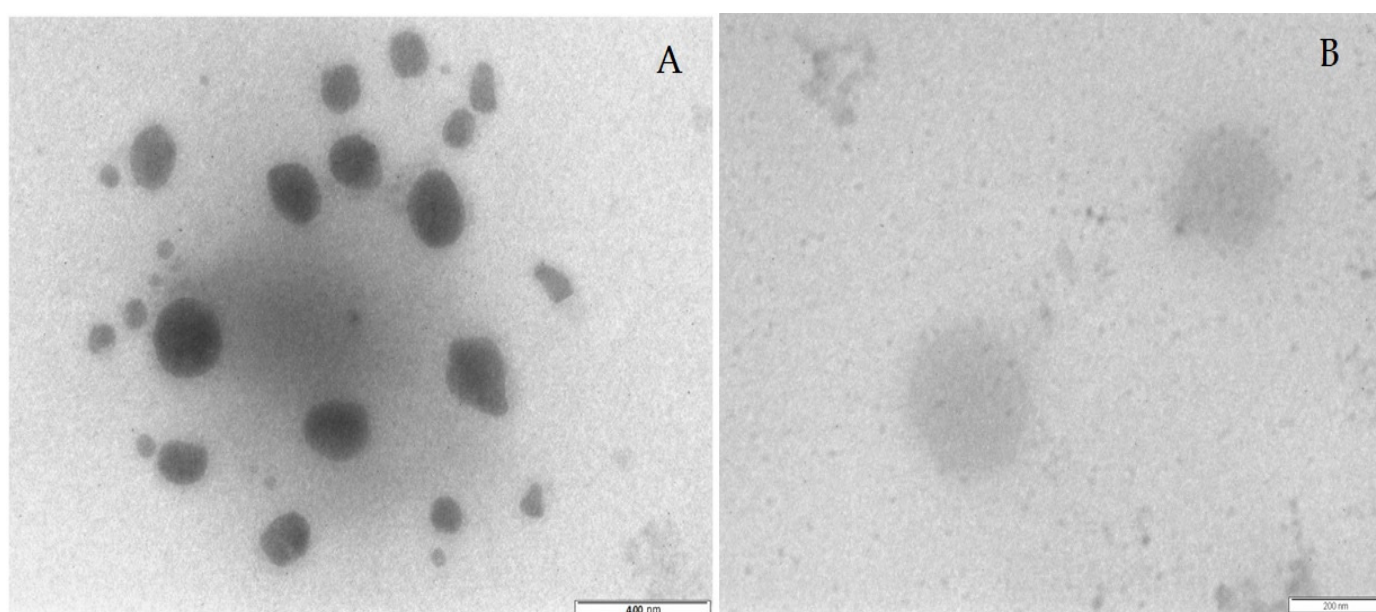

Figure 5. (**A**) Morphology (TEM) studies of prepared quercetin-loaded micelles, (**B**) Focused view of particle at high magnification.

3.6. In Vitro Cytotoxicity Studies

The *in vitro* cytotoxicity of quercetin nanogel was evaluated and compared with pure quercetin on MCF-7 cells using an *in vitro* SRB assay. The study results showed that nanogel has superior cytotoxicity than quercetin. As shown in Table 2, the concentration of quercetin causing the total inhibition of cell growth (TGI) in the MCF 7 cell line for the nanogel was found to be 79.29μg/mL, whereas for quercetin, TGI was found to be 96.73μg/mL. The TGI value for ADR, that is, Adriamycin (standard), was found to be 60.21 μg/mL. The study results reveals that the formulation showed significant reduction in TGI value (* $p < 0.00002$) compared with Adriamycin (standard), and growth inhibition 50% (GI 50) values for quercetin was observed to be 29 μg/mL, whereas for formulation and Adriamycin, GI 50 was found to be <10, indicating improved cytotoxic potential in the formulation, which may be attributed to increased cellular uptake due to its nano-micellar structure. Figure 6 shows photo images wherein Figure 6A shows that denser MCF-7 cells are of normal control, while Figure 6B–D are of treatment with quercetin, the formulation, and standard Adriamycin, respectively, which appear to be less dense and round. This improved activity may be due to the improved internalization of micellar structure within cells with reduction in particle size and micellar structure. Pluronic-F68, an excipient used in formulation development, has well-demonstrated non-cytotoxicity through various experimental studies [46,47] and

does not contribute to cytotoxicity. Despite the repulsive electrostatic interactions with the cell membrane, negatively charged micelles can be internalized by cells through various mechanisms like endocytosis, particularly clathrin-mediated or caveolae-mediated endocytosis, which is the primary pathway for their uptake. Additionally, the enhanced permeability and retention (EPR) effect in tumors allows for better micelle accumulation in cancer cells. Studies showed that modifications like PEGylation or functionalizing micelles with specific ligands can improve their uptake, demonstrating that surface charge alone is not the sole factor influencing internalization [48].

Table 2. In vitro cytotoxicity studies on MCF 7 cell line (n = 6).

	Drug Concentration (μg/mL)	
MCF 7	**TGI**	**GI50**
Formulation	79.29 $\pm$ 1.11 *	<10
Quercetin	96.73 $\pm$ 1.89 **	29 $\pm$ 0.41
Adriamycin (standard)	60.21 $\pm$ 0.91	<10

Values are expressed as mean $\pm$ SEM, n = 6, by using one-way ANOVA, followed by Tukey's multiple comparison test. * $p < 0.00002$, ** $p < 0.0007$, ns: non-significant.
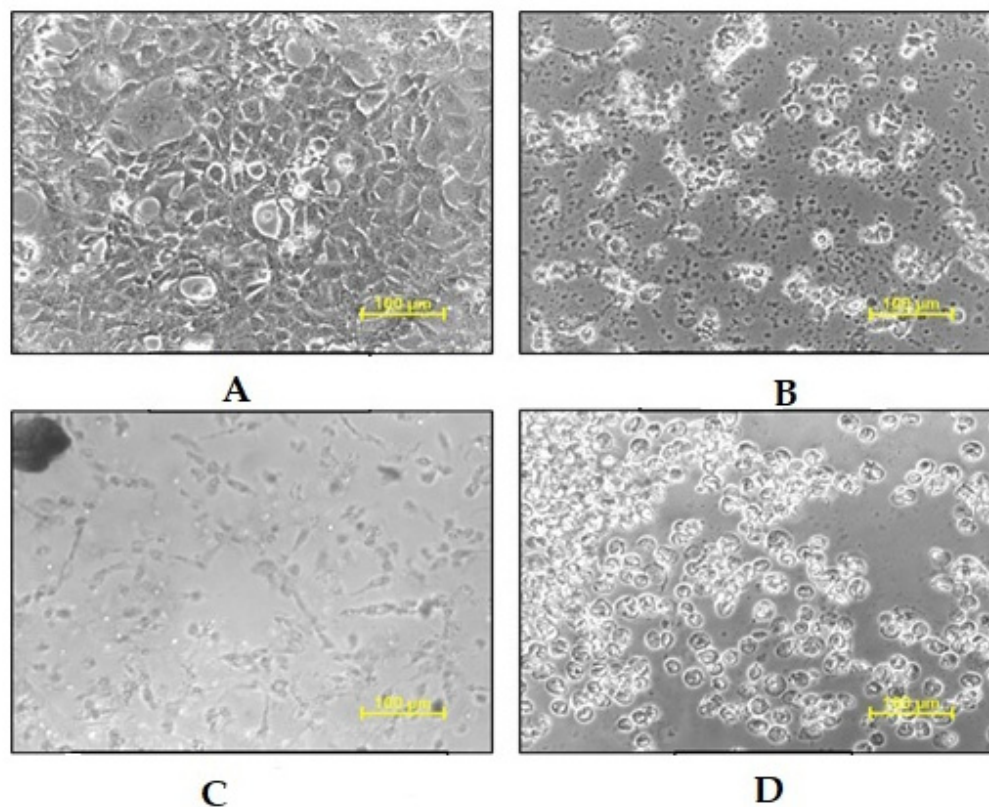

Figure 6. Microscopic images of in vitrocytotoxicity studies on (**A**) MCF-7 control, (**B**) quercetin, (**C**) formulation, and (**D**) Adriamycin (standard).

3.7. Evaluation of Quercetin Micellar Nanogel

Yellowish transparent uniform textured gel was formulated with the incorporation of quercetin-loaded polymeric nanomicelles. The gel viscosity was observed to be increased with high pH adjusted in the range of 5.5–6.5. Viscosity was observed in the range of 200–800 pa. s (gm/s). The spreadability of the quercetin micellar nanogel was found to be 2.9 gm. Cm/sec. The release pattern of quercetin from developed gel formulation is observed as shown in Figure 7. The study results show that quercetin diffuses freely in

the solution at about 96.12± 0.43% in 2 h, whereas quercetin release from the formulation showed a burst release of 33.20 ± 0.86% at the initial phase in first 1.5 h and sustained release 96.11 ± 0.75% up to 8 h. Three fundamental mechanisms, erosion, diffusion, and degradation, aid in the loaded medication release from the micellar gel. Sustained release may have been brought on by the drug's diffusion.
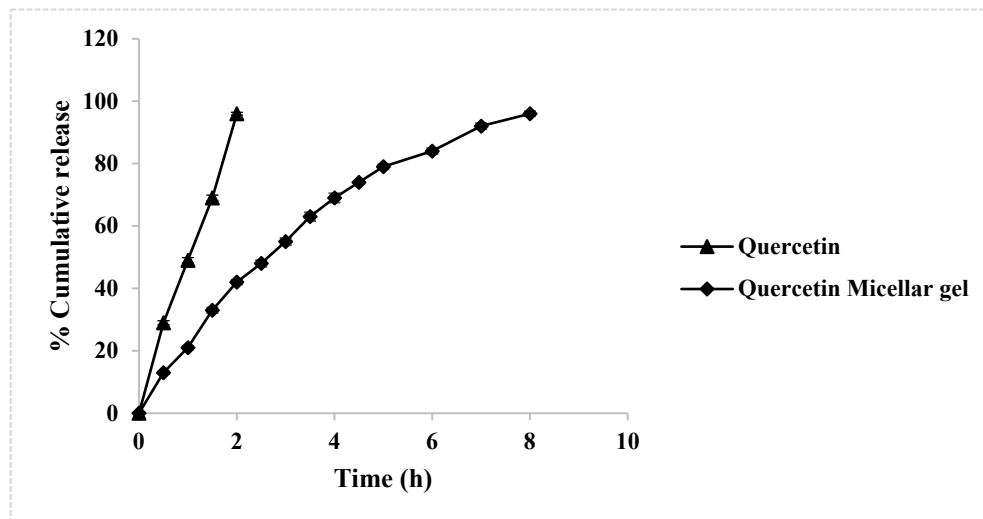

Figure 7. *In vitro* release study.

4. Conclusions

The developed quercetin micellar gel optimized formulation revealed desirable characteristics in terms of a size of 180.26 ± 2.4 nm, surface charge of −13.5 mV, and entrapment efficiency of 78.4 ± 1.2%. The formulation also showed 33.20 ± 0.86% burst release in the first 1.5 hr followed by a sustained release of 96.11 ± 0.75% up to 8 h. The overall study results demonstrated favorable formulation characteristics that may also have an impact on the resulting good physical and chemical stability. The desirable drug release pattern and improved cytotoxicity potential on MCF-7 cells compared with quercetin may improve biopharmaceutical performance. Overall, the present formulation strategy may be promising for the delivery of quercetin in topical cancer therapy.

Abbreviations

The following abbreviations are used in this manuscript:

CMC	Critical micellar concentration
PK	Pharmacokinetics
PLGA	Poly (lactic-co-glycolic acid)
PF 68	Pluronic F 68
PDI	Polydispersibility Index
TEM	Transmission electron microscopy

References

1. Mahomoodally, M.F.; Sadeer, N.; Edoo, M.; Venugopala, K.N. The Potential Application of Novel Drug Delivery Systems for Phytopharmaceuticals and Natural Extracts–Current Status and Future Perspectives. *Mini-Rev. Med. Chem.* **2021**, *21*, 2731–2746. [CrossRef] [PubMed]

2. Sindhu, R.K.; Verma, R.; Salgotra, T.; Rahman, H.; Shah, M.; Akter, R.; Murad, W.; Mubin, S.; Bibi, P.; Qusti, S.; et al. Impacting the Remedial Potential of Nano Delivery-Based Flavonoids for Breast Cancer Treatment. *Molecules* **2021**, *26*, 5163. [CrossRef] [PubMed]

3. Krol, W. The dietary flavonolfisetin enhances the apoptosis-inducing potential of TRAIL in prostate cancer cells. *Int. J. Oncol.* **2011**, *39*, 771–779.

4. Kapare, H.S.; Giram, P.S.; Raut, S.S.; Gaikwad, H.K.; Paiva-Santos, A.C. Formulation Development and Evaluation of Indian Propolis Hydrogel for Wound Healing. *Gels* **2023**, *9*, 375. [CrossRef]

5. Joseph, A.; Shanmughan, P.; Balakrishnan, A.; Maliakel, B. Enhanced Bioavailability and Pharmacokinetics of a Natural Self-Emulsifying Reversible Hybrid-Hydrogel System of Quercetin: A Randomized Double-Blinded Comparative Crossover Study. *ACS Omega* **2022**, *7*, 46825–46832. [CrossRef]

6. Singh, S.; Grewal, S.; Sharma, N.; Behl, T.; Gupta, S.; Anwer, K.; Vargas-De-La-Cruz, C.; Mohan, S.; Bungau, S.G.; Bumbu, A. Unveiling the Pharmacological and Nanotechnological Facets of Daidzein: Present State-of-the-Art and Future Perspectives. *Molecules* **2023**, *28*, 1765. [CrossRef]

7. Tang, J.; Xu, N.; Ji, H.; Liu, H.; Wang, Z.; Wu, L. Eudragit nanoparticles containing genistein: Formulation, development, and bioavailability assessment. *Int. J. Nanomed.* **2011**, *6*, 2429–2435. [CrossRef]

8. Tawornchat, P.; Pattarakankul, T.; Palaga, T.; Intasanta, V.; Wanichwecharungruang, S. Polymerized Luteolin Nanoparticles: Synthesis, Structure Elucidation, and Anti-Inflammatory Activity. *ACS Omega* **2021**, *6*, 2846–2855. [CrossRef]

9. Zhai, G.; Guo, C.; Tan, Q.; Liu, W. Preparation and evaluation of quercetin-loaded lecithin-chitosan nanoparticles for topical delivery. *Int. J. Nanomed.* **2011**, *6*, 1621–1630. [CrossRef]

10. Bhattacharya, T.; Soares, G.A.B.E.; Chopra, H.; Rahman, M.M.; Hasan, Z.; Swain, S.S.; Cavalu, S. Applications of Phy-to-Nanotechnology for the Treatment of Neurodegenerative Disorders. *Materials* **2022**, *15*, 804. [CrossRef]

11. Hosseini, A.; Razavi, B.M.; Banach, M.; Hosseinzadeh, H. Quercetin and metabolic syndrome: A review. *Phytother. Res.* **2021**, *35*, 5352–5364. [CrossRef] [PubMed]

12. Wang, Z.X.; Ma, J.; Li, X.Y.; Wu, Y.; Shi, H.; Chen, Y.; Lu, G.; Shen, H.M.; Lu, G.D.; Zhou, J. Quercetin induces p53-independent cancer cell death through lysosome activation by the transcription factor EB and Reactive Oxygen Species-dependent ferroptosis. *Br. J. Pharmacol.* **2021**, *178*, 1133–1148. [CrossRef] [PubMed]

13. Vincent, M.; Lehoux, J.; Desmarty, C.; Moine, E.; Legrand, P.; Dorandeu, C.; Simon, L.; Durand, T.; Brabet, P.; Crauste, C.; et al. A novel lipophenol quercetin derivative to prevent macular degeneration: Intravenous and oral formulations for preclinical pharmacological evaluation. *Int. J. Pharm.* **2023**, *651*, 123740. [CrossRef] [PubMed]

14. Jia, H.; Zhang, Y.; Si, X.; Jin, Y.; Jiang, D.; Dai, Z.; Wu, Z. Quercetin Alleviates Oxidative Damage by Activating Nuclear Factor Erythroid 2-Related Factor 2 Signaling in Porcine Enterocytes. *Nutrients* **2021**, *13*, 375. [CrossRef]

15. Tian, R.; Yang, Z.; Lu, N.; Peng, Y.-Y. Quercetin, but not rutin, attenuated hydrogen peroxide-induced cell damage via heme oxygenase-1 induction in endothelial cells. *Arch. Biochem. Biophys.* **2019**, *676*, 108157. [CrossRef]

16. Dhanaraj, T.; Mohan, M.; Arunakaran, J. Quercetin attenuates metastatic ability of human metastatic ovarian cancer cells via modulating multiple signaling molecules involved in cell survival, proliferation, migration and adhesion. *Arch. Biochem. Biophys.* **2021**, *701*, 108795. [CrossRef]

17. Maruszewska, A.; Tarasiuk, J. Quercetin Triggers Induction of Apoptotic and Lysosomal Death of Sensitive and Multidrug Resistant Leukaemia HL60 Cells. *Nutr. Cancer* **2021**, *73*, 484–501. [CrossRef]

18.　Almatroodi, S.A.; Alsahli, M.A.; Almatroudi, A.; Verma, A.K.; Aloliqi, A.; Allemailem, K.S.; Khan, A.A.; Rahmani, A.H. Potential Therapeutic Targets of Quercetin, a Plant Flavonol, and Its Role in the Therapy of Various Types of Cancer through the Modulation of Various Cell Signaling Pathways. *Molecules* **2021**, *26*, 1315. [CrossRef]

19.　Wei, X.; Song, M.; Li, W.; Huang, J.; Yang, G.; Wang, Y. Multifunctional nanoplatforms co-delivering combinatorial dual-drug for eliminating cancer multidrug resistance. *Theranostics* **2021**, *11*, 6334–6354. [CrossRef]

20.　Lei, C.S.; Hou, Y.C.; Pai, M.H.; Lin, M.T.; Yeh, S.L. Effects of quercetin combined with anticancer drugs on metasta-sis-associated factors of gastric cancer cells: In vitro and in vivo studies. *J. Nutr. Biochem.* **2018**, *51*, 105–113. [CrossRef]

21.　Jamshidi-Mouselou, M.S.; Hashemi, A.; Jamshidi-Mouselou, M.S.; Farkhondeh, T.; Pourhanifeh, M.H.; Samarghandian, S. Application of Quercetin and its Novel Formulations in the Treatment of Malignancies of Central Nervous System: An Up-dated Review of Current Evidence based on Molecular Mechanisms. *Curr. Med. Chem.* **2024**, *31*, 4180–4198. [CrossRef] [PubMed]

22.　Guo, H.; Ding, H.; Tang, X.; Liang, M.; Li, S.; Zhang, J.; Cao, J. Quercetin induces pro-apoptotic autophagy via SIRT1/AMPK signaling pathway in human lung cancer cell lines A549 and H1299 in vitro. *Thorac Cancer* **2021**, *12*, 1415–1422. [CrossRef] [PubMed]

23.　Chen, X.; McClements, D.J.; Zhu, Y.; Chen, Y.; Zou, L.; Liu, W.; Cheng, C.; Fu, D.; Liu, C. Enhancement of the solubility, stability and bioaccessibility of quercetin using protein-based excipient emulsions. *Food Res. Int.* **2018**, *114*, 30–37. [CrossRef] [PubMed]

24.　Li, Y.; Yao, J.; Han, C.; Yang, J.; Chaudhry, M.T.; Wang, S.; Liu, H.; Yin, Y. Quercetin, Inflammation and Immunity. *Nutrients* **2016**, *8*, 167. [CrossRef]

25.　Ahmad, N.; Ahmad, R.; Ahmad, F.J.; Ahmad, W.; Alam, M.A.; Amir, M.; Ali, A. Poloxamer-chitosan-based Naringenin nanoformulation used in brain targeting for the treatment of cerebral ischemia. *Saudi J. Biol. Sci.* **2020**, *27*, 500–517. [CrossRef]

26.　Tran, T.H.; Guo, Y.; Song, D.H.; Bruno, R.S.; Lu, X.L. Quercetin-containing self-nanoemulsifying drug delivery system for improving oral bioavailability. *J. Pharm. Sci.* **2014**, *103*, 840–852. [CrossRef]

27.　Rasaie, S. Nano phytosomes of quercetin: A promising formulation for fortification of food products with antioxidants. *Pharm. Sci.* **2014**, *10*, 96–101.

28.　Singh, A.; Dutta, P.; Kumar, H.; Kureel, A.K.; Rai, A.K. Synthesis of chitin-glucan-aldehyde-quercetin conjugate and evaluation of anticancer and antioxidant activities. *Carbohydr. Polym.* **2018**, *193*, 99–107. [CrossRef]

29.　Zhao, M.-H.; Yuan, L.; Meng, L.-Y.; Qiu, J.-L.; Wang, C.-B. Quercetin-loaded mixed micelles exhibit enhanced cytotoxic efficacy in non-small cell lung cancer in vitro. *Exp. Ther. Med.* **2017**, *14*, 5503–5508. [CrossRef]

30.　Ravichandiran, V.; Masilamani, K.; Senthilnathan, B.; Maheshwaran, A.; Wong, T.W.; Roy, P. Quercetin-Decorated Curcumin Liposome Design for Cancer Therapy: In-Vitro and In-Vivo Studies. *Curr. Drug Deliv.* **2017**, *14*, 1053–1059. [CrossRef]

31.　Cecerska-Heryć, E.; Wiśniewska, Z.; Serwin, N.; Polikowska, A.; Goszka, M.; Engwert, W.; Michałów, J.; Pękała, M.; Budkowska, M.; Michalczyk, A.; et al. Can Compounds of Natural Origin Be Important in Chemoprevention? Anticancer Properties of Quercetin, Resveratrol, and Curcumin—A Comprehensive Review. *Int. J. Mol. Sci.* **2024**, *25*, 4505. [CrossRef] [PubMed]

32.　Przybylski, P.; Lewińska, A.; Rzeszutek, I.; Błoniarz, D.; Moskal, A.; Betlej, G.; Deręgowska, A.; Cybularczyk-Cecotka, M.; Szmatoła, T.; Litwinienko, G.; et al. Mutation Status and Glucose Availability Affect the Response to Mitochondria-Targeted Quercetin Derivative in Breast Cancer Cells. *Cancers* **2023**, *15*, 5614. [CrossRef] [PubMed]

33.　Lin, R.; Piao, M.; Song, Y.; Liu, C. Quercetin Suppresses AOM/DSS-Induced Colon Carcinogenesis through Its Anti-Inflammation Effects in Mice. *J. Immunol. Res.* **2020**, *2020*, 9242601. [CrossRef] [PubMed]

34.　Sun, Y.; Bai, Y.; Liu, S.; Cui, S.; Xu, P. Thermosensitive Micelles Gel to Deliver Quercetin Locally for Enhanced Antibreast Cancer Efficacy: An In Vitro Evaluation. *IET Nanobiotechnology* **2023**, *2023*, 7971492. [CrossRef] [PubMed]

35.　Bose, A.; Burman, D.R.; Sikdar, B.; Patra, P. Nanomicelles: Types, properties and applications in drug delivery. *IET Nanobiotechnology* **2021**, *15*, 19–27. [CrossRef]

36.　An, J.Y.; Yang, H.S.; Park, N.R.; Koo, T.-S.; Shin, B.; Lee, E.H.; Cho, S.H. Development of Polymeric Micelles of Oleanolic Acid and Evaluation of Their Clinical Efficacy. *Nanoscale Res. Lett.* **2020**, *15*, 133. [CrossRef]

37.　Rijcken, C.; Soga, O.; Hennink, W.; van Nostrum, C. Triggered destabilisation of polymeric micelles and vesicles by changing polymers polarity: An attractive tool for drug delivery. *J. Control. Release* **2007**, *120*, 131–148. [CrossRef]

38.　Mehan, N.; Kumar, M.; Bhatt, S.; Shankar, R.; Kumari, B.; Pahwa, R.; Kaushik, D. Self-Assembly Polymeric Nano Micelles for the Futuristic Treatment of Skin Cancer and Phototoxicity: Therapeutic and Clinical Advancement. *Crit. Rev. Ther. Drug Carr. Syst.* **2022**, *39*, 79–95. [CrossRef]

39.　Taymouri, S.; Varshosaz, J.; Hassanzadeh, F.; Javanmard, S.H.; Dana, N. Optimisation of processing variables effective on self-assembly of folate targeted Synpronic-based micelles for docetaxel delivery in melanoma cells. *IET Nanobiotechnology* **2015**, *9*, 306–313. [CrossRef]

40.　Trinh, H.M.; Joseph, M.; Cholkar, K.; Mitra, R.; Mitra, A.K. Nanomicelles in Diagnosis and Drug Delivery. In *Emerging Nanotechnologies for Diagnostics, Drug Delivery and Medical Devices*; Elsevier: Amsterdam, The Netherlands, 2017; pp. 45–58.

41. Munot, N.; Kandekar, U.; Giram, P.S.; Khot, K.; Patil, A.; Cavalu, S. A comparative study of quercetin-loaded nanocochleates and liposomes: Formulation, characterization, assessment of degradation and in vitro anticancer potential. *Pharmaceutics* **2022**, *14*, 1601. [CrossRef]

42. Kapare, H.S.; Lohidasan, S.; Sinnathambi, A.; Mahadik, K. Formulation Development of Folic Acid Conjugated PLGA Nanoparticles for Improved Cytotoxicity of Caffeic Acid Phenethyl Ester. *Pharm. Nanotechnol.* **2021**, *9*, 111–119. [CrossRef] [PubMed]

43. Shitole, A.A.; Sharma, N.; Giram, P.; Khandwekar, A.; Baruah, M.; Garnaik, B.; Koratkar, S. LHRH-conjugated, PEGylated, poly-lactide-co-glycolidenanocapsulesfor targeted delivery of combinational chemotherapeutic drugs Docetaxel and Quercetin for prostate cancer. *Mater. Sci. Eng. C Mater. Biol. Appl.* **2020**, *114*, 111035. [CrossRef] [PubMed]

44. Patil, P.H.; Wankhede, P.R.; Mahajan, H.S.; Zawar, L.R. Aripiprazole-Loaded Polymeric Micelles: Fabrication, Optimization and Evaluation using Response Surface Method. *Recent Pat. Drug Deliv. Formul.* **2018**, *12*, 53–64. [CrossRef] [PubMed]

45. Tilawat, M.; Bonde, S. Curcumin and quercetin loaded nanocochleates gel formulation for localized application in breast cancer therapy. *Heliyon* **2023**, *9*, e22892. [CrossRef] [PubMed]

46. Noor, N.S.; Kaus, N.H.M.; Szewczuk, M.R.; Hamid, S.B.S. Formulation, Characterization and Cytotoxicity Effects of Novel Thymoquinone-PLGA-PF68 Nanoparticles. *Int. J. Mol. Sci.* **2021**, *22*, 9420. [CrossRef]

47. Khaliq, N.U.; Lee, J.; Kim, S.; Sung, D.; Kim, H. Pluronic F-68 and F-127 Based Nanomedicines for Advancing Combination Cancer Therapy. *Pharmaceutics* **2023**, *15*, 2102. [CrossRef]

48. Foroozandeh, P.; Aziz, A.A. Insight into Cellular Uptake and Intracellular Trafficking of Nanoparticles. *Nanoscale Res. Lett.* **2018**, *13*, 339. [CrossRef]